

1 **Finding decodable information that is read out in behaviour**

2

3 Tijl Grootswagers^{1,2,3,*} (tijl.grootswagers@sydney.edu.au)

4 Radoslaw M. Cichy⁴ (rmcichy@zedat.fu-berlin.de)

5 Thomas A. Carlson^{1,2} (thomas.carlson@sydney.edu.au)

6

7 *corresponding author

8 ¹School of Psychology, University of Sydney, NSW 2006, Australia

9 ²ARC Centre of Excellence in Cognition and its Disorders, NSW 2109, Australia

10 ³Department of Cognitive Science, Macquarie University, NSW 2109, Australia

11 ⁴Department of Education and Psychology, Freie Universität Berlin, 14195 Berlin, Germany

12

13 **Acknowledgements**

14 This research was supported by an Australian Research Council Future Fellowship (FT120100816)

15 and an Australian Research Council Discovery project (DP160101300) awarded to T.A.C., and

16 a German Research Foundation grant (CI-241/1-1) awarded to R.M.C. The authors acknowledge

17 the University of Sydney HPC service for providing High Performance Computing resources. The

18 authors declare no competing financial interests.

19

20 **Abstract**

21

22 Multivariate decoding methods applied to neuroimaging data have become the standard in
23 cognitive neuroscience for unravelling statistical dependencies between brain activation patterns
24 and experimental conditions. The current challenge is to demonstrate that information decoded
25 as such by the experimenter is in fact used by the brain itself to guide behaviour. Here we
26 demonstrate a promising approach to do so in the context of neural activation during object
27 perception and categorisation behaviour. We first localised decodable information about visual
28 objects in the human brain using a spatially-unbiased multivariate decoding analysis. We then
29 related brain activation patterns to behaviour using a machine-learning based extension of signal
30 detection theory. We show that while there is decodable information about visual category
31 throughout the visual brain, only a subset of those representations predicted categorisation
32 behaviour, located mainly in anterior ventral temporal cortex. Our results have important
33 implications for the interpretation of neuroimaging studies, highlight the importance of relating
34 decoding results to behaviour, and suggest a suitable methodology towards this aim.

35

36 **1 Introduction**

37 Multivariate pattern analysis (MVPA), also called brain decoding, are a powerful tool to establish
38 statistical dependencies between experimental conditions and brain activation patterns (Carlson,
39 Schrater, & He, 2003; Cox & Savoy, 2003; Haxby et al., 2001; Haynes, 2015; Kamitani & Tong,
40 2005; Kriegeskorte, Goebel, & Bandettini, 2006). In these analyses, an implicit assumption often
41 made by experimenters is that if information can be decoded, then this information is used by the
42 brain in behaviour (de-Wit, Alexander, Ekroll, & Wagemans, 2016; Ritchie, Kaplan, & Klein, 2017).
43 However, the decoded information could be different (e.g., epiphenomenal) from the signal that is
44 relevant for the brain (de-Wit et al., 2016; Williams, Dang, & Kanwisher, 2007), highlighting the
45 need to relate decoded information to behaviour. To address this, previous work has correlated
46 decoding performances to behavioural accuracies (e.g., Bouton et al., 2018; Freud, Culham, Plaut,
47 & Behrmann, 2017; Naselaris, Kay, Nishimoto, & Gallant, 2011; Raizada, Tsao, Liu, & Kuhl, 2010;
48 van Bergen, Ji Ma, Pratte, & Jehee, 2015; Walther, Caddigan, Fei-Fei, & Beck, 2009; Williams et al.,
49 2007). However, this does link decoding and behaviour at the level of individual experimental
50 conditions. Another approach has been to compare neural and behavioural similarity structures
51 (e.g., Bracci & op de Beeck, 2016; Cohen, Dennett, & Kanwisher, 2016; Grootswagers, Kennedy,
52 Most, & Carlson, 2017; Haushofer, Livingstone, & Kanwisher, 2008; Mur et al., 2013; Proklova,
53 Kaiser, & Peelen, 2016; Wardle, Kriegeskorte, Grootswagers, Khaligh-Razavi, & Carlson, 2016).
54 While this approach allows to link behaviour and brain patterns at the level of single experimental
55 conditions, it is unclear how this link carries over to decision making behaviour such as
56 categorisation.

57

58 Recently, a novel methodological approach, called the distance-to-bound approach (Ritchie &
59 Carlson, 2016), has been proposed to connect brain activity directly to perceptual decision-making
60 behaviour at the level of individual experimental conditions. The rationale behind this approach

61 (Carlson, Ritchie, Kriegeskorte, Durvasula, & Ma, 2014; Kiani, Cueva, Reppas, & Newsome, 2014;
62 Philiastides & Sajda, 2006; Ritchie & Carlson, 2016) is that for decision-making tasks, the brain
63 applies a decision boundary to a neural activation space (DiCarlo & Cox, 2007). Similarly, MVPA
64 classifiers fit multi-dimensional hyperplanes to separate a neural activation space. The distance of
65 the input to a decision boundary reflects the ambiguity of the evidence for the decision (Green &
66 Swets, 1966) and thus predicts reaction times (Ashby, 2000; Ashby & Maddox, 1994). If for a
67 decision task (e.g., categorisation), the brain uses the same information as the MVPA classifier,
68 then the classifier's hyperplane reflects the brain's decision boundary. This in turn predicts that
69 distance to the classifier's hyperplane negatively correlates with reaction times for the decision
70 task. Carlson et al. (2014) demonstrated the promise of the distance-to-bound approach in a
71 region of interest based analysis using fMRI. Here we go beyond this work by using the distance-
72 to-bound method and a spatially unbiased approach to create maps of where in the brain
73 information can be used to guide behaviour.

74

75 **2 Materials and Methods**

76 In this study, we separately localised information that is decodable, and information that is
77 suitably formatted to guide behaviour in the context of decodable information about visual
78 objects and object categorisation behaviour. To ensure robustness and generality of our results,
79 we analysed in parallel two independent fMRI datasets (Cichy et al., 2014, 2016), with different
80 stimulus sets, and in relation to partly overlapping categorisation behaviours. Overall, this allowed
81 us to investigate the relationship between decodable information from brain activity and
82 categorisation behaviour for six different distinctions: animate versus inanimate, faces versus
83 bodies, human versus animal, tools versus not tools, food versus not food, and transport versus
84 not food. Note that the negative 'not-X' category was defined as all stimuli that did fall into one of
85 the aforementioned classes. Categorisation reaction times for those stimuli were collected on

86 Amazon's Mechanical Turk. In this section, we describe the two-step searchlight procedure used
87 to create decoding and correlation maps of areas involved in visual object categorisation.

88

89 **2.1 Experimental design**

90 **Stimuli**

91 Stimuli for experiment 1 consisted of 92 visual objects, segmented on a white background (Figure
92 1A). Stimuli consisted of animate and inanimate objects. The animate objects could be further
93 divided into faces, bodies, humans and animals. Inanimate objects consisted of natural (e.g.,
94 plants or fruits) and man-made items (e.g., tools or houses). The stimulus set for experiment 2
95 consisted of 118 visual objects on natural backgrounds (Figure 1C). A small proportion of the
96 objects (27) were animate. The inanimate objects included subcategories such as tools, or food
97 items. In both experiments, participants were presented with the visual object stimuli while
98 performing an orthogonal task at fixation. Stimuli were displayed at 2.9° (Experiment 1) and 4.0°
99 (Experiment 2) visual angle with 500 ms duration. Images were displayed (overlaid with a grey
100 fixation cross) for 500 ms in random order.

101

102 **fMRI recordings**

103 The first experiment (Cichy et al., 2014) had high resolution fMRI coverage of the ventral visual
104 stream (Figure 1B) from 15 participants with a 2 mm isotropic voxel resolution. The second
105 experiment (Cichy et al., 2016) had whole brain from 15 participants with a 3 mm isotropic voxel
106 resolution. In both experiments, at the start of a session, structural images were obtained using a
107 standard T₁-weighted sequence. fMRI data were aligned and coregistered to the T1 structural
108 image, and then normalized to a standard MNI template. General linear models were used to
109 compute t-values for each stimulus (92 and 118, respectively) against baseline.

110

111 **Reaction time data**

112 We obtained reaction times for the stimuli in multiple different categorisation contrasts (Figure
113 1A&B). For experiment 1, these were animate versus inanimate, face versus body, and human
114 versus animal. For experiment 2, we tested animate versus inanimate, tool versus not tool, food
115 versus not food, and transport versus not transport. The RTs were collected using Amazons
116 Mechanical Turk (MTurk). For each of the categorisation contrasts, 50 unique participants
117 performed a categorisation task using the same stimuli as were used in collecting the fMRI data.
118 Participants were instructed to “Categorise the images as fast and accurate as possible using the
119 following keys: (z for X, m for Y)”, where X and Y would be replaced with the relevant categories
120 (e.g., animate and inanimate) for the contrast. On each trial, an image was presented for 500ms,
121 followed by a black screen until the participant’s response (Figure 1C). The presentation order of
122 the stimuli was randomized and stimuli did not repeat. This resulted in 50 reaction time values per
123 exemplar (one for each participant). Each participant’s reaction times were z-scored. Next, we
124 computed the median reaction time (across participants) for each exemplar. This resulted in one
125 reaction time value per exemplar, which were used in the rest of the study.

126

127 **2.2 Statistical Analysis**

128 **Searchlight procedure**

129 For each categorisation contrast and subject, we used a searchlight approach (Haynes et al., 2007;
130 Kriegeskorte et al., 2006) to create maps of decoding accuracy and of correlations between
131 distance to the classifier boundary and categorisation reaction times. In contrast to pre-defined
132 ROI’s, which are used to test a-priori hypotheses about the spatial origin of information in the
133 brain, the searchlight results in a spatially unbiased map of decodable information. An overview of
134 the approach is presented in Figure 1D.

135

136 To create the decoding accuracy maps, we used a standard searchlight decoding approach
137 (Grootswagers, Wardle, & Carlson, 2017; Haynes, 2015; Kriegeskorte et al., 2006; Pereira, Mitchell,
138 & Botvinick, 2009), as implemented in the CoSMoMMPA decoding toolbox (Oosterhof, Connolly, &
139 Haxby, 2016). In detail, at each spatial location (voxel) in an fMRI image, a support vector machine
140 (SVM) was used to classify visual object category based on local brain patterns, resulting in a map
141 of classification accuracies. We then determined the subset of the locations at which brain
142 patterns were suitably formatted for read-out by the brain using the distance-to-bound approach
143 (Ritchie & Carlson, 2016) in a second searchlight analysis. Analogous to the decoding analysis, at
144 each voxel, an SVM was trained to classify visual objects. Diverging at this point from the decoding
145 approach we did not test the classifier, but rather obtained the distance for each exemplar to the
146 hyperplane set by the SVM. We then correlated those distances to reaction times acquired in
147 separate categorisation tasks. The contribution of each category was assessed individually, by
148 performing the correlations separately for the two sides of the categorisation (e.g., one
149 correlation for animate and one for inanimate exemplars). For each categorisation task this
150 resulted in two correlation maps per subject. The maps of decoding accuracy and correlations
151 were assessed for significance at the group level using sign-rank tests for random-effects
152 inference. The results were thresholded at $p < 0.05$, using the false discovery rate (FDR; (Benjamini
153 & Hochberg, 1995)) to correct for multiple comparisons at the voxel level.

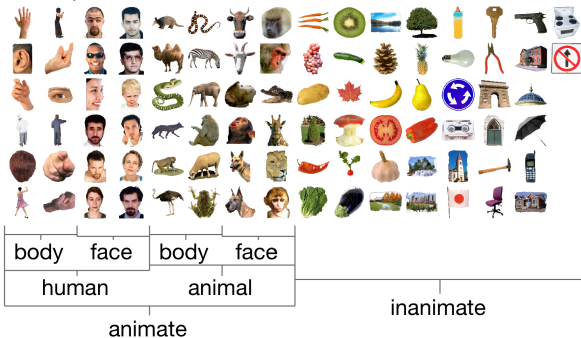
154

155 **Relating the results to topographical locations of the visual system**

156 For each of the categorisation contrasts, we identified the locations of the significant voxels with
157 respect to ROIs of the visual system. The significant voxels in the decoding maps and correlation
158 maps were compared to probabilistic topographic maps of visual processing areas (Wang,
159 Mruczek, Arcaro, & Kastner, 2015), which represent for each voxel the visual area with the highest
160 probability. A percentage score for each ROI was then computed, reflecting the percentage of

161 voxels in this ROI that were significant at the group level. We obtained a bootstrapped distribution
 162 of percentage scores for each ROI by repeating this procedure 10,000 times, while randomly
 163 sampling the subjects with replacement and recomputing the group level statistics. We report the
 164 5th, 50th and 95th percentiles of this distribution. This approach allows quantifying the difference
 165 between the number of decoding voxels and correlation voxels per visual ROI.

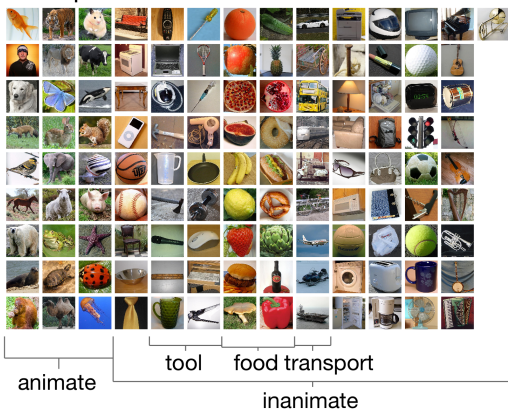
A Experiment 1: stimuli



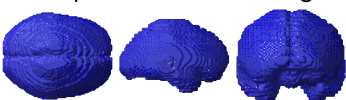
B Experiment 1: coverage



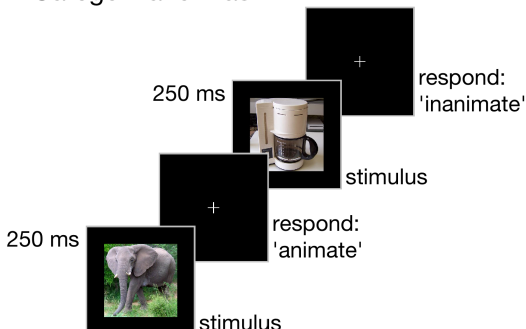
C Experiment 2: stimuli



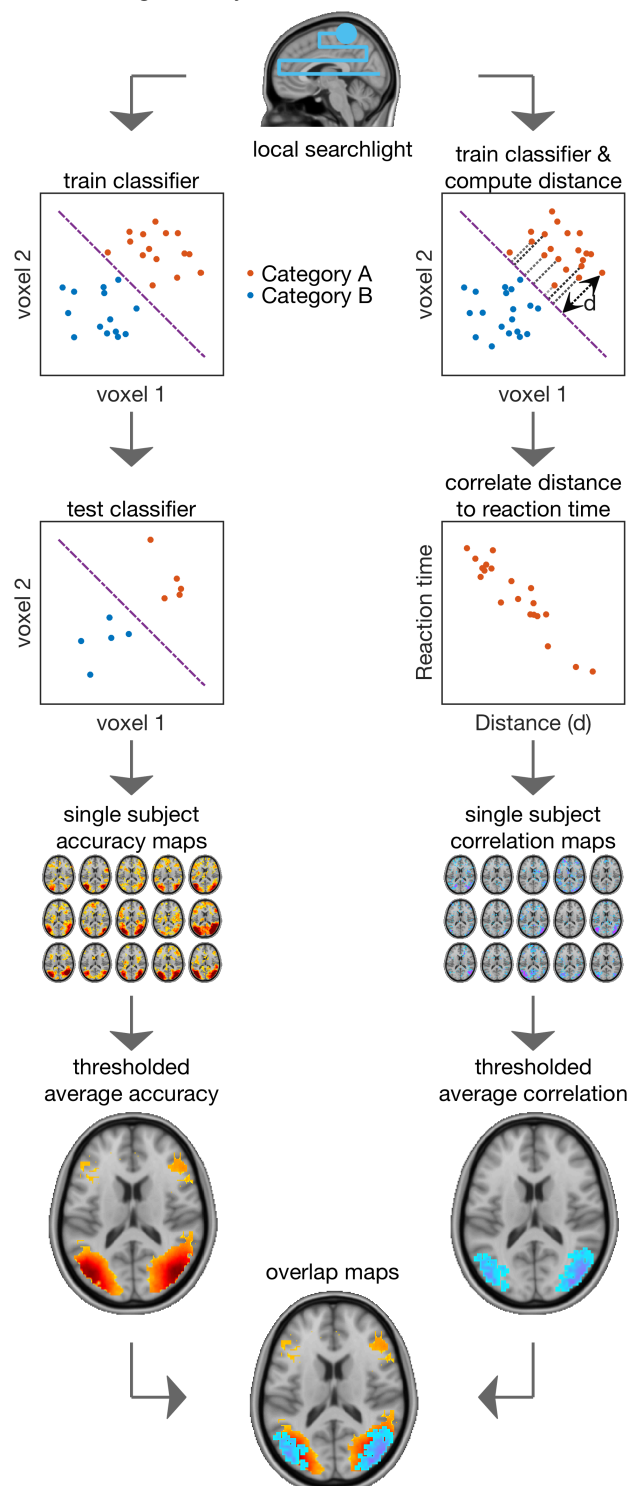
D Experiment 2: coverage



E Categorization task



F Searchlight analysis



166

167 **Figure 1. General experimental rationale.** Stimuli (A,C) used to map fMRI brain responses and
168 brain coverage (B,C) for fMRI study 1 and 2 respectively. E. Acquisition of reaction times on object
169 categorisation tasks. Reaction times for categorisation contrasts were collected in a different pool
170 of participants than the ones participating in the fMRI experiment. On each trial, a stimulus was
171 displayed for 250ms, and participants categorised it into two categories (exemplarily here:
172 animate vs inanimate) by pressing one of two keys. F. The two-partite approach to separately
173 localize decodable information and information that is suitable for read out in behaviour. For both
174 parts, a local cluster of neighbouring voxels (i.e., searchlight) was used to train a linear support
175 vector machine (SVM) on an image category classification task (e.g., animacy). To localize
176 decodable information, the classifier was tested on left-out data, storing the classification
177 accuracy at the centre voxel of the searchlight. To localise information that was suitably formatted
178 for read-out in a categorisation task, the distances of objects to the classifier hyperplane were
179 correlated with the reaction times for the same object images on the same classification task.
180 Repeated for every voxel, this resulted for each subject in one map of decoding accuracies and
181 one of correlations. For visualisation, significant correlation voxels were superimposed on
182 significant decoding accuracy voxels, each showing group average values in significant voxels.

183

184 **3 Results**

185 We examined the relationship between decodable information and information that is suitably
186 formatted for read-out by the brain in the context of decodable information about visual objects
187 and object categorisation behaviour. We determined the relationship between decodable
188 information and behaviour separately. First, we determined where information about objects is
189 present in brain patterns using decoding in a standard fMRI searchlight decoding analysis (Haynes
190 et al., 2007; Kriegeskorte et al., 2006). We then determined the subset of the locations at which
191 brain patterns were suitably formatted for read-out by the brain using the distance-to-bound
192 approach (Ritchie & Carlson, 2016) in a second searchlight analysis. The subject-specific
193 searchlight results were subjected to inference statistics at the group level using one-sided sign
194 rank tests and thresholded at $p < 0.05$ (fdr-corrected for multiple comparisons across voxels).

195

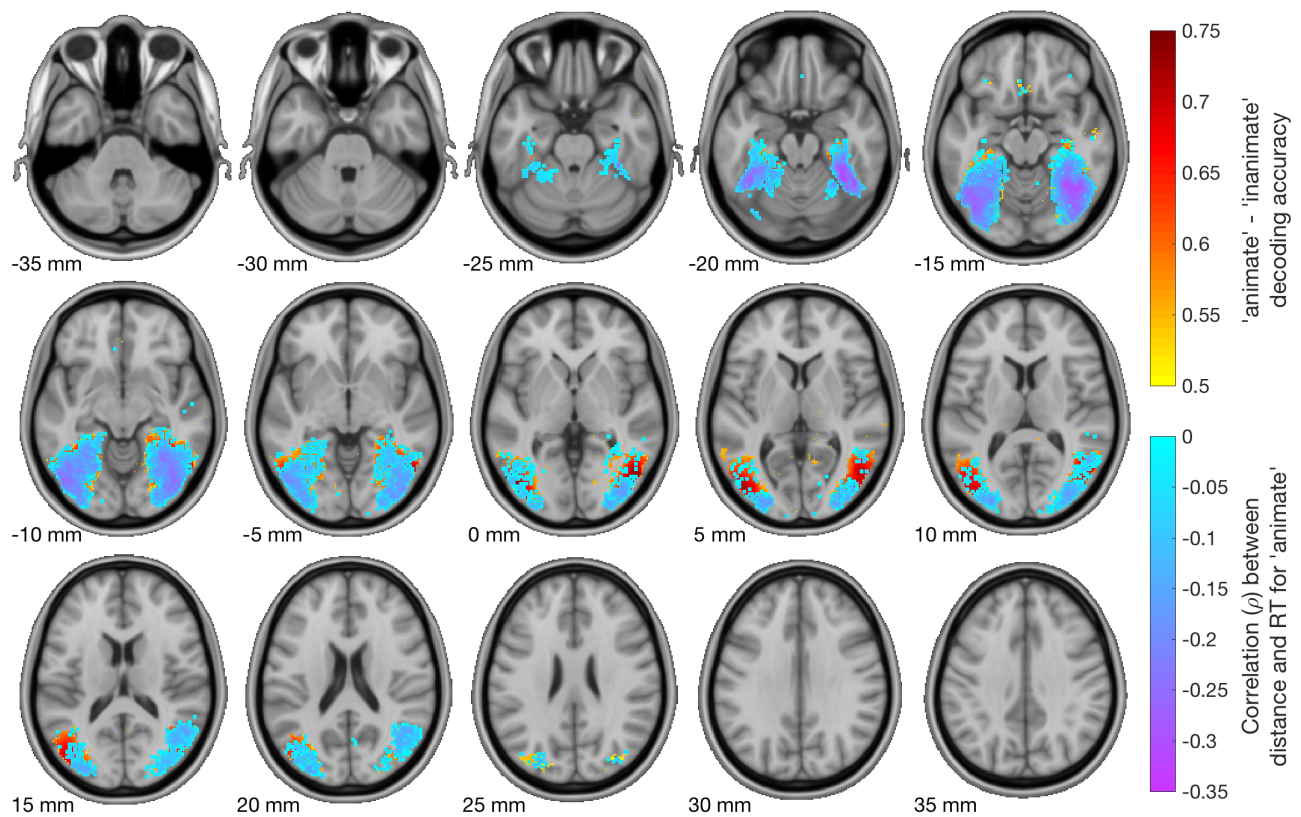
196 **3.1 A subset of locations that have decodable information about animacy also had information**
197 **suitably formatted for animacy categorisation behaviour**

198 Animacy is a pervasive and basic object property according to which any object can be classified as
199 animate or inanimate (Caramazza & Shelton, 1998). Previous studies have shown that the division
200 of animate versus inanimate objects is reflected in the large-scale architecture of high-level visual
201 areas such as the ventral temporal cortex (VTC) (Caramazza & Shelton, 1998; Grill-Spector &
202 Weiner, 2014; Kriegeskorte et al., 2008), However, it has also been shown that animacy can be
203 decoded not only from VTC, but from the whole ventral visual stream (Cichy et al., 2016; Grill-
204 Spector & Weiner, 2014; Long, Yu, & Konkle, 2017). Furthermore, categorical object responses
205 have also been found in the dorsal visual stream (Bracci, Daniels, & op de Beeck, 2017; Freedman
206 & Assad, 2006; Konen & Kastner, 2008) and in frontal areas (Freedman, Riesenhuber, Poggio, &
207 Miller, 2001, 2003). This prompts the question of where in the visual system object
208 representations are suitably formatted for read-out by the brain for animacy decisions.

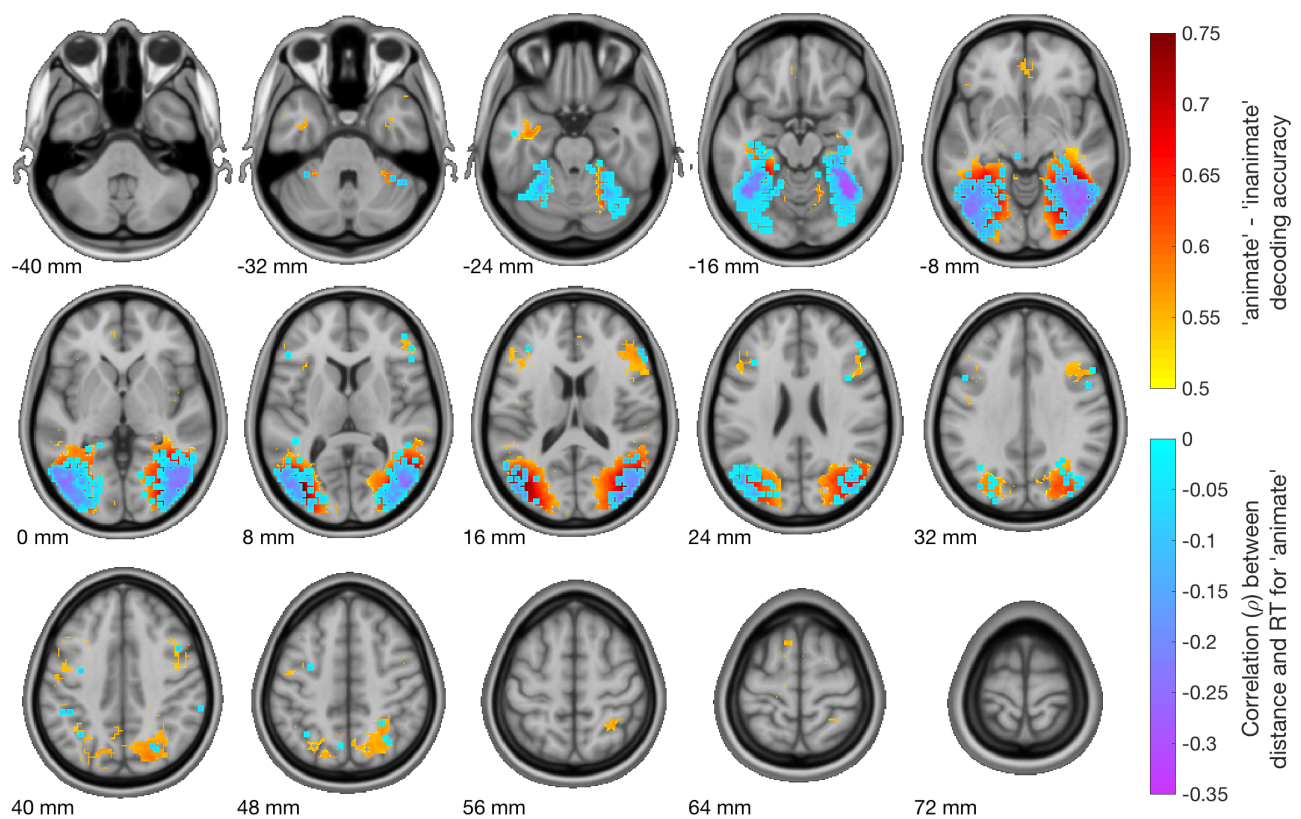
209
210 Corroborating previous studies, we found decodable information about animacy in the entire
211 ventral visual stream from the occipital pole to anterior ventral temporal cortex (Figure 2AB, Table
212 1AD, $N = 15$, one-sided sign-rank test, $p < 0.05$ *fdr*-corrected). In addition, we found decodable
213 information in dorsal and prefrontal cortex (Figure 2B) in experiment 2 which had full brain
214 coverage. Localising the brain representations suitable to guide animacy categorisation behaviour
215 (using the distance-to-bound approach) revealed convergent evidence across experiments that
216 only a subset of voxels containing decodable information fulfilled this criterion. In detail, distance-
217 RT-correlations for animate objects were strongest in the high-level regions of the ventral and the
218 dorsal stream. For inanimate objects, we found no voxels with significant distance-RT-correlations
219 (Carlson et al., 2014; Grootswagers, Ritchie, Wardle, Heathcote, & Carlson, 2017).

220

A Experiment 1: animate - inanimate



B Experiment 2: animate - inanimate



221

222 **Figure 2. Relationship between decodable information and categorisation behaviour for**
223 **animacy. A.** In experiment 1, decodable animacy information (hot colours) was found throughout
224 the ventral stream. A correlation between distance to the classifier boundary and reaction time for

225 animate stimuli (cool colours) was found in a subset of these areas. **B.** The results of the analysis
 226 for experiment 2 corroborated these findings, and showed decodable information in prefrontal
 227 areas and in the dorsal visual stream. Correlations between distance and reaction time were also
 228 present in the dorsal stream. Visualizations show average results across subjects in significant
 229 voxels (N=15, sign-rank test, $p < 0.05$ *fdr*-corrected) projected onto axial slices of a standard T_1
 230 image in MNI space.

Contrast	#significant voxels	Max/min	uncorr. p-value	X	Y	Z
A) decoding 'animate' vs 'inanimate' (exp 1)	11745	0.80	0.0000	36	-52	-15
Distance-RT-correlation 'animate'	6410	-0.38	0.0000	38	-58	-19
Distance-RT-correlation 'inanimate'	0	-0.16	0.0021	-48	-58	5
B) decoding 'human' vs 'animal'	4863	0.69	0.0000	22	-90	-13
Distance-RT-correlation 'human'	0	-0.29	0.0002	30	-58	-15
Distance-RT-correlation 'animal'	0	-0.17	0.0072	48	-46	-4
C) decoding 'face' vs 'body'	10661	0.84	0.0000	44	-78	-10
Distance-RT-correlation 'face'	226	-0.32	0.0000	40	-76	-15
Distance-RT-correlation 'body'	0	-0.20	0.0000	-54	-68	16
D) decoding 'animate' vs 'inanimate' (exp 2)	8824	0.80	0.0000	36	-55	-11
Distance-RT-correlation 'animate'	2015	-0.34	0.0000	51	-73	-2
Distance-RT-correlation 'inanimate'	0	-0.12	0.0002	-21	-43	-2
E) decoding 'tool' vs 'not tool'	0	0.58	0.0002	-30	-94	7
Distance-RT-correlation 'tool'	0	-0.25	0.0013	-33	-13	19
Distance-RT-correlation 'not tool'	0	-0.24	0.0001	-33	-52	-17
F) decoding 'transport' vs 'not transport'	0	0.59	0.0001	33	-94	1
Distance-RT-correlation 'transport'	0	-0.32	0.0003	15	50	4
Distance-RT-correlation 'non-transport'	0	-0.18	0.0000	-33	-55	-14
G) decoding 'food' vs 'not food'	1092	0.62	0.0002	36	-55	-14
Distance-RT-correlation 'food'	0	-0.16	0.0177	-18	26	-5
Distance-RT-correlation 'not food'	154	-0.13	0.0002	27	-40	-14

231 **Table 1. Results for all categorisation contrasts.** For all categorisation contrasts, we report the
 232 number of significant voxels (after correction for multiple comparisons), its peak value (maximum
 233 for decoding or minimum for distance-RT-correlation) and uncorrected p-value, and the peak's
 234 location in MNI-XYZ coordinates.

235 **3.2 The proportion of region-specific representations suitably formatted for behaviour increases** 236 **along the ventral stream and decreases along the dorsal stream**

237 We next explicitly determined the degree to which representations in single brain regions within
238 the ventral and dorsal streams are suitably formatted for behaviour. For this we parcellated the
239 cortex (Figure 3A) using a probabilistic topographic map of visual processing areas (Wang et al.,
240 2015). For each region, we calculated the ratio between the number of significant voxels in the
241 decoding analysis and the total number of voxels, so that a high ratio indicates that a large part of
242 a region contains object representations with categorical information. Similarly, we calculated the
243 ratio between the number of significant voxels in the distance-to-bound analysis and the total
244 number of voxels. Here, a high ratio indicates that a large part of a region contains object
245 representations that are suitably formatted for read out in a categorisation task.

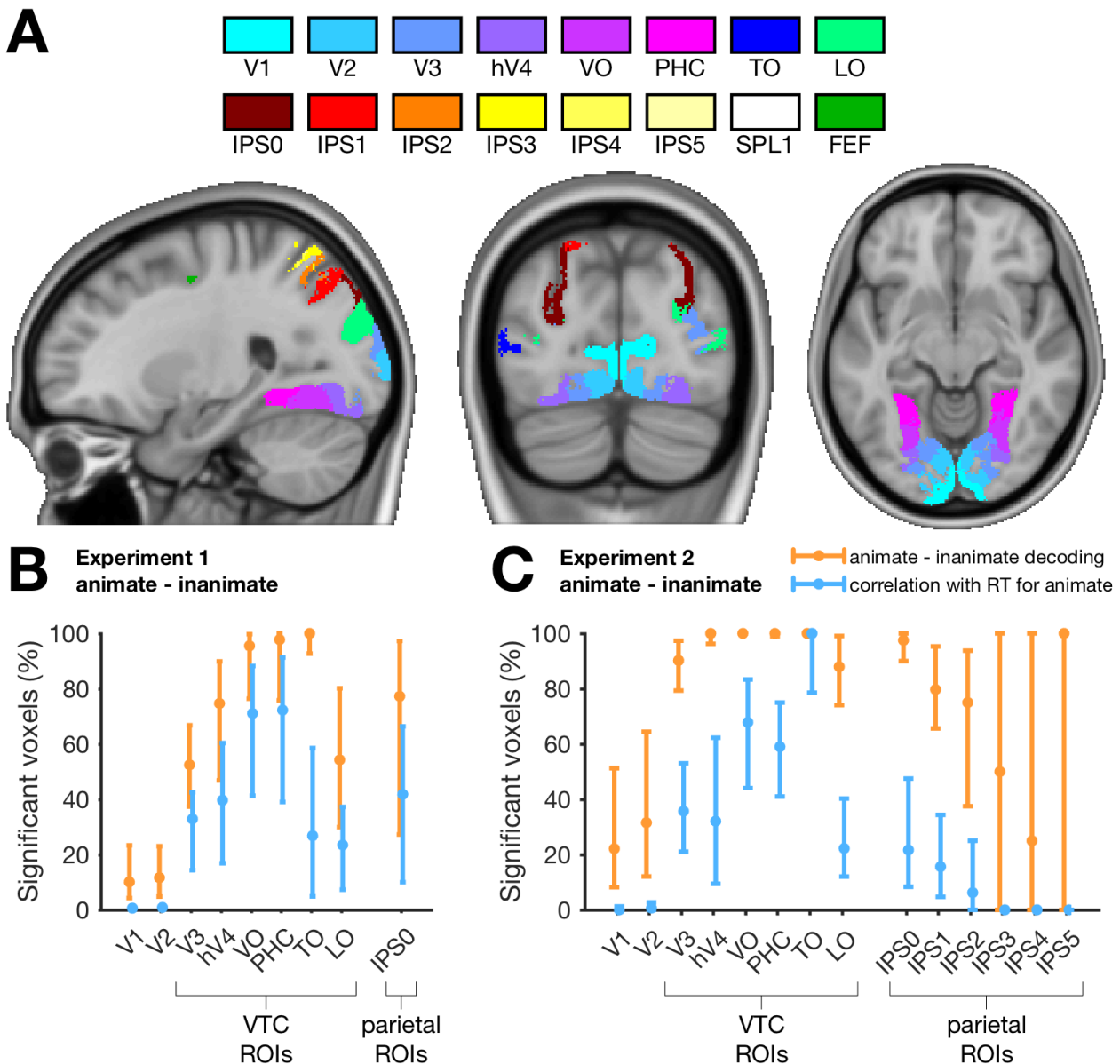
246

247 In the ventral stream, we observed a systematic increase in ratio with processing stage, from early
248 visual areas to high-level visual areas, with highest ratios in ventral occipital (VO) and
249 parahippocampal (PHC) cortex (Figure 3 B&C). In contrast, in the dorsal stream we observed a
250 systematic decrease of the correlation ratio with processing stage. In addition, significant animacy
251 decoding information was found in similar proportions in the ventral-temporal areas as in lateral-
252 occipital areas, however, the proportion of voxels with information suitable for categorisation was
253 lower in lateral-occipital areas. This is consistent with the notion that while both these regions
254 contain object representations, the VTC contains location-invariant representations which are
255 essential for object categorisation (Cichy et al., 2013; Haushofer et al., 2008; Schwarzlose, Swisher,
256 Dang, & Kanwisher, 2008; Williams et al., 2007).

257

258 In sum, these results show that representations along the ventral stream are shaped for optimal
259 read-out of categorical information (Cichy et al., 2013; Grill-Spector & Weiner, 2014). In contrast,

260 representations in the dorsal stream might be shaped for the read-out in different tasks (Bracci et
 261 al., 2017; Freud et al., 2017). These results also suggest that intermediate stages along the ventral
 262 and dorsal streams may be similar or partly shared, as suggested by the similar ratios of
 263 information suitable for read-out.
 264



265
 266 **Figure 3. Quantifying the decodable information in visual areas and their contribution to**
 267 **categorisation behaviour.** **A.** Locations of topographical ROIs of the visual system (Wang et al.,
 268 2015), containing early visual cortex (EVC) areas V1 and V2, mid-level areas V3 and hV4, high level
 269 ventral occipital (VO) and parahippocampal cortex (PHC), temporal occipital (TO) and lateral
 270 occipital (LO) areas, areas in the intra-parietal sulcus (IPS), the superior parietal lobule (SPL), and

271 the frontal eye fields (FEF). **B-C.** The ratio between significant voxels in an ROI and the size of the
272 ROI. Orange points show the ratio of voxels within the ROI that had significant animacy decoding
273 performance. Blue points show the ratio of voxels with a significant correlation between distance
274 to the hyperplane and RT for 'animate'. The lower, middle and upper points on these lines indicate
275 5th, 50th, and 95th percentiles (bootstrapping of participants 10,000 times). These results quantify
276 the increasing contribution of early to late areas in the ventral visual stream to animacy
277 categorisation behaviour.

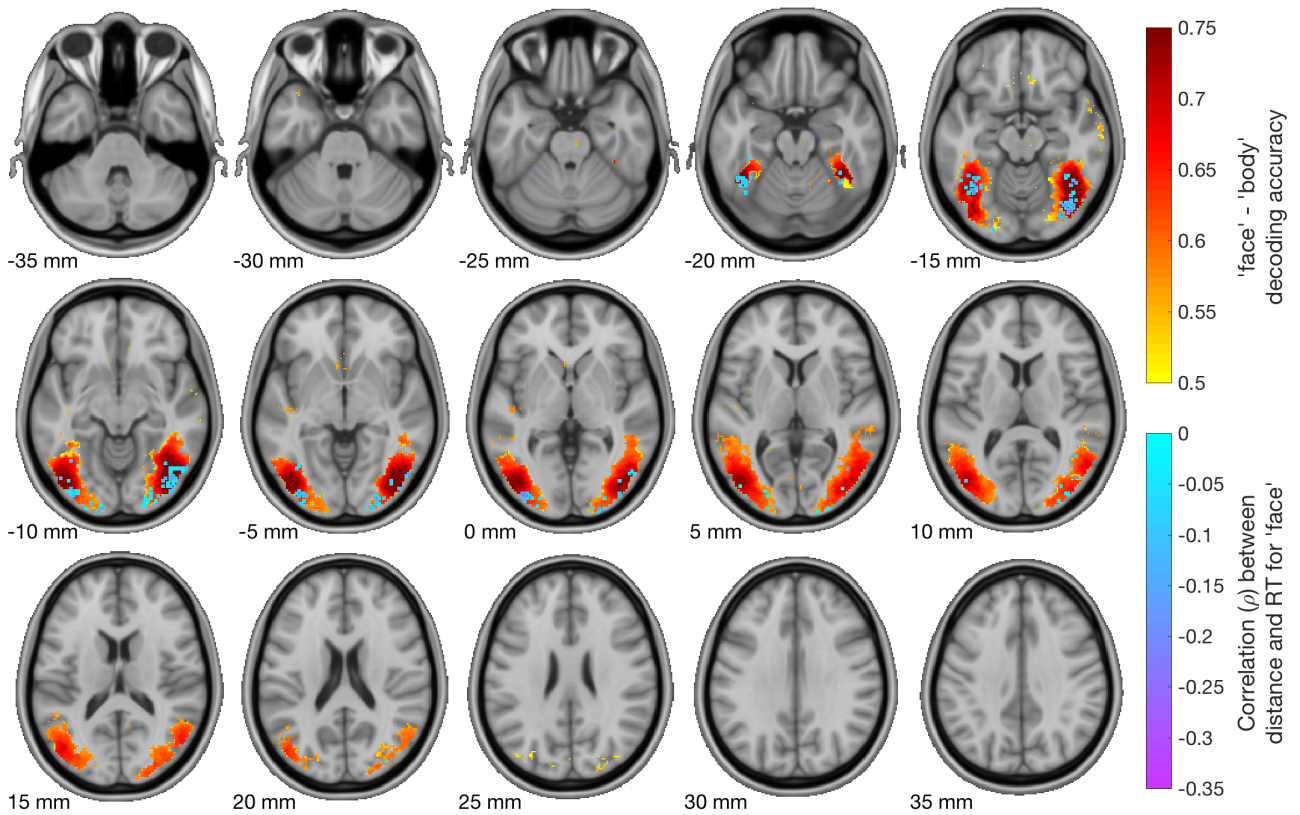
278

279 **3.3 Decodable information about subordinate categorisation tasks is also suitably formatted for** 280 **categorisation behaviour**

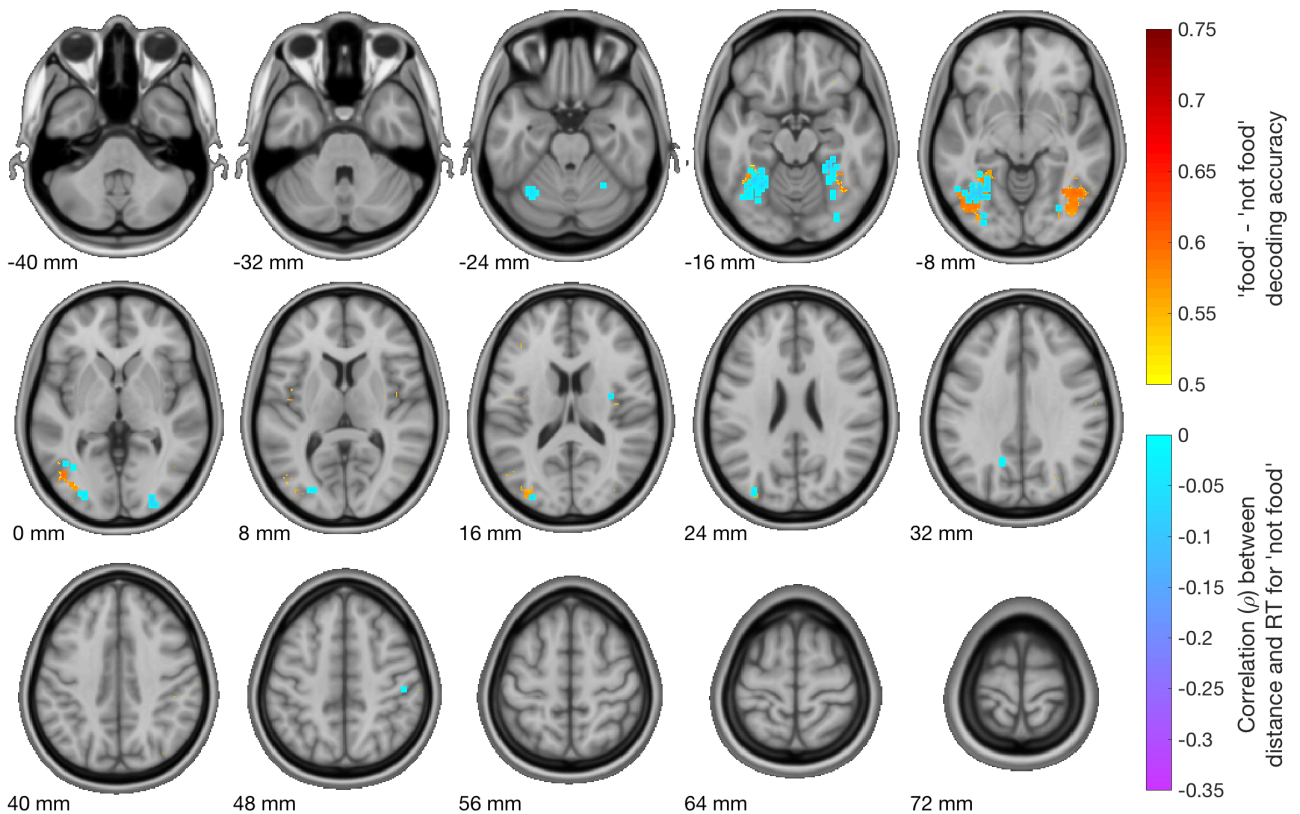
281 While animacy categorisation may be based on large-scale representational differences in the
282 visual brain (Carlson, Tovar, Alink, & Kriegeskorte, 2013; Downing, Chan, Peelen, Dodds, &
283 Kanwisher, 2006; Grill-Spector & Weiner, 2014; Kriegeskorte et al., 2008), subordinate
284 categorisation tasks (e.g., faces, bodies, tools) may depend more on fine grained patterns in focal
285 brain regions (Downing, Jiang, Shuman, & Kanwisher, 2001; Downing & Peelen, 2016; Kanwisher,
286 McDermott, & Chun, 1997). Here, we tested whether decodable information about subordinate
287 category membership is also suitably formatted for read out in respective categorisation tasks. We
288 tested two subordinate contrasts for experiment 1: face versus body, and human versus animal
289 using the same general procedure as for animacy. We found that both contrasts were decodable
290 (Table 1B-C). We found a significant correlation between distance to the classifier hyperplane and
291 reaction time for faces in the face versus body task (Figure 4A). Of the subordinate categorisation
292 contrasts in experiment 2 (food, transport or tool versus everything else), transport and tool
293 versus everything else were not significantly decodable information nor had they significant
294 correlations (Table 1E-F). Food versus not food resulted in significant decodable information, and
295 significant distance-RT correlations were present for this contrast in the 'not food' category
296 (Figure 4B, Table 1G). Taken together, for some subordinate categorisation contrasts that were

297 decodable, we were successful in localising brain patterns suitably formatted for read-out in
298 behaviour.

A Experiment 1: face - body



B Experiment 2: food - not food



299

300 **Figure 4. Relationship between decodable information and behaviour for subordinate**
301 **categorisation tasks. A.** In experiment 1, decodable face versus body information (hot colours)
302 was found in the entire ventral stream. A distance-RT-correlation for the face stimuli (cool colours)
303 was found in a subset of these areas. **B.** In experiment 2, food versus not food was decodable in
304 some areas in the ventral visual stream. A distance-RT-correlation for the 'not food' stimuli was
305 found in a subset of these areas. Visualisations show average results across subjects in significant
306 voxels (N=15, sign-rank test, $p < 0.05$ *fdr*-corrected) projected onto axial slices of a standard T_1
307 image in MNI space.

308

309 **4 Discussion**

310 **4.1 Dissociating between decodable information and information that is used in behaviour**

311 The aim of this study was to examine where in the brain decodable information is suitably
312 formatted for read-out by the brain in behaviour. We found that only a subset of information that
313 is decodable could be related to behaviour using the distance-to-bound approach, which argues
314 for a partial dissociation between decodable information and information that is relevant for
315 behaviour. This speaks to a current challenge in neuroimaging, which is to show that information
316 visible to the experimenter is in fact used by the brain (de-Wit et al., 2016; Ritchie et al., 2017). To
317 illustrate, consider the question about what regions are used by the brain to perform an object
318 animacy categorisation task (DiCarlo, Zoccolan, & Rust, 2012; Grill-Spector & Weiner, 2014). On its
319 own, the result of the animacy decoding searchlight might be interpreted as the brain using
320 animacy information from anywhere in the ventral stream. However, when investigating this
321 interpretation directly using the distance-RT-correlation results, it becomes clear that object
322 animacy information is represented for read-out in mid- and high-level visual areas only.

323

324 It is important to note that not finding a correlation between distance to the classifier hyperplane
325 and RT does not imply that the information revealed using the decoding approach is irrelevant or
326 epiphenomenal. The distance-to-bound approach taken here makes specific assumptions about

327 the brain's read-out process, such as distance in representational space as the measure for
328 evidence, and a rank-order relationship between distance and reaction time (Ritchie & Carlson,
329 2016). Other assumptions follow from those imposed by the decoding approach, such as the
330 binary classification, the size of the searchlight radius, and the choice of classifier. For example, it
331 could be that the representations are relevant in a different task (Grootswagers, Ritchie, et al.,
332 2017; Ritchie & Carlson, 2016), or that read-out involves pooling over larger spatial scales or
333 multiple brain areas. Therefore, the current approach only allows the positive inference on the
334 level of suitability of decoded information for behaviour in the context of the current task and
335 decoding parameters. On the other hand, a correlation with behaviour still does not prove that
336 the information is used by the brain, but it shows that the information is at least formatted in a
337 way that is suitable to be used by the brain for decisions. Future work can use causal measures
338 (e.g., TMS) targeting the areas highlighted in the current results.

339

340 **4.2 The contribution of ventral and dorsal visual regions to categorisation behaviour**

341 We found that neural representations suitably formatted for behaviour in categorisation were
342 most prominently located in the anterior regions of the VTC. This corroborates previous studies
343 (Afraz, Kiani, & Esteky, 2006; Carlson et al., 2014; Hong, Yamins, Majaj, & DiCarlo, 2016; Hung,
344 Kreiman, Poggio, & DiCarlo, 2005), and reinforces the tight link between VTC and visual
345 categorisation behaviour. In these areas, our results provide converging evidence for the (implicit)
346 assumption made in neuroimaging studies, which is that information that is available to the
347 experimenter is also available for read out by the brain in behaviour (cf. de-Wit et al., 2016).

348

349 However, we found that correlations between distance to boundary and RT were not restricted to
350 anterior regions of the VTC, but were also prominent in V3 and hV4. This is consistent with the
351 view that lower level visual features encoded in mid-level visual regions could aid faster read-out

352 of category information. V4 is thought of as an intermediate stage of visual processing that
353 aggregates lower level visual features into invariant representations (Riesenhuber & Poggio,
354 1999). It has been proposed that direct pathways from V4 to decision areas allow the brain to
355 exploit visual feature cues for fast responses to ecologically important stimuli (Hong et al., 2016;
356 Kirchner & Thorpe, 2006; Thorpe, Fize, & Marlot, 1996), such as identifying faces (Crouzet,
357 Kirchner, & Thorpe, 2010; Honey, Kirchner, & VanRullen, 2008). An alternative possibility is that
358 read out is not happening directly from V4, but its representational structure is shaped by the low-
359 level feature differences in animacy. This structure is then largely preserved when it is
360 communicated to more anterior areas, leading to similar distance-RT-correlations. Both of these
361 accounts are also consistent with recent findings that show differential responses for object
362 categories in mid-level visual areas (Long et al., 2017; Proklova et al., 2016). The extent to which
363 visual features contribute to the read-out process could be further investigated by using the
364 approach from this study with different stimulus sets that control for these features (Kaiser,
365 Azzalini, & Peelen, 2016; Long et al., 2017; Proklova et al., 2016).

366

367 We found that distance-RT-correlations were also present in early parietal areas. The classical
368 view is that the ventral and dorsal visual streams are recruited for different function (Ungerleider
369 & Mishkin, 1982). However, areas in the ventral and dorsal streams have been found to exhibit
370 similar object-selective responses (Freud et al., 2017; Konen & Kastner, 2008; Sereno & Maunsell,
371 1998; Silver & Kastner, 2009). Consistent with this, we found similar RT-distance-correlations in
372 mid-level areas in the ventral and dorsal streams. However, our results also showed that the
373 proportion of correlations decreased along the dorsal stream, while they increased along the
374 ventral stream. This suggests that representations in the ventral and dorsal streams undergo
375 similar transformations at first, and then diverge for different goals.

376

377 **4.3 Without a task, neural object representations in the VTC are formatted for read-out in**
378 **categorisation decisions**

379 Here, the fMRI participants performed an orthogonal task, and were not actively categorising.
380 Despite this, categorisation reaction times could still be predicted from representations in the
381 visual stream. This highlights that, without a categorisation task, information in the visual system
382 is represented in a way that is suitable for read out in behaviour (Carlson et al., 2014; Ritchie,
383 Tovar, & Carlson, 2015). In addition, the orthogonal task in the scanner has the advantage that it
384 avoids RT- and difficulty confounds (see e.g., Hebart & Baker, 2017; Woolgar, Golland, & Bode,
385 2014). Future studies might use the distance-to-bound approach with participants actively
386 performing the same task in the scanner, where we predict that areas involved in the decision
387 making and execution processes would contain information that correlates with reaction time. For
388 example, some areas preferentially represent task-relevant information, such as areas in the
389 prefrontal cortex (Duncan, 2001; Jackson, Rich, Williams, & Woolgar, 2016; Woolgar, Jackson, &
390 Duncan, 2016), and in the parietal stream (Bracci et al., 2017; Freedman & Assad, 2016; Jeong &
391 Xu, 2016). In the absence of an animacy categorisation task, one would predict that animacy
392 information would not be strongly represented in these areas. Yet, our results showed that
393 animacy information can be decoded from prefrontal and parietal areas when participants
394 perform an orthogonal task. However, our results also showed that the animacy information in
395 these areas was not predictive of reaction time. This again highlights the dissociation between
396 information that can be decoded, and information that is suitable for read out in behaviour. A
397 prediction that follows from this is that performing an active object categorisation task in the
398 scanner would change the representations in these task-relevant areas so that they become
399 predictive of reaction time (Bugatus, Weiner, & Grill-Spector, 2017; McKee, Riesenhuber, Miller, &
400 Freedman, 2014).

401

402 **4.4 Asymmetric distance-RT-Correlations in binary categorisation tasks**

403 In both experiments, we found correlations between distance and reaction time for animate
404 stimuli, but none for the inanimate stimuli. This is consistent with previous work (Carlson et al.,
405 2014; Grootswagers, Ritchie, et al., 2017; Ritchie et al., 2015), which argued that this discrepancy
406 might be caused by inanimate being a negatively defined category (i.e., “not animate”). Under this
407 hypothesis the animacy categorisation task can be performed by collecting evidence for animate
408 stimuli and responding inanimate only when not enough evidence was accumulated after a certain
409 amount of time. Here, we tested a prediction of this hypothesis by contrasting two positively
410 defined categories, face versus body, and found that there was a distance-RT-correlation only for
411 faces. This goes against the notion of the negative definition of inanimate as the main reason for a
412 lack of correlation. However, it still is possible that observers still treated these tasks as ‘A’ or ‘NOT
413 A’, with ‘A’ being the category that is easiest to detect (Grootswagers, Ritchie, et al., 2017). For
414 example, perceptual evidence for a face would be easier to obtain than evidence for a body-part,
415 as faces share low level visual features (Crouzet & Thorpe, 2011; Honey et al., 2008; Wu, Crouzet,
416 Thorpe, & Fabre-Thorpe, 2015). Thus, while not explicitly specified as a negative category, it could
417 have been treated as such.

418

419 This suggests that the binary categorisation might be an unnatural way of approaching human
420 categorisation behaviour in the real world. Other operationalisations such as picture naming or
421 visual search may be better suited to capture the relevant behaviours (cf. Krakauer, Ghazanfar,
422 Gomez-Marin, Maclver, & Poeppel, 2017). Still, it is important to note that the binary task matches
423 the brain decoding task performed by the classifier. The above-chance decoding accuracy in the
424 brain decoding task is commonly interpreted as a similar dichotomy in the brain’s representation
425 that the brain can use in a decision. However, when only the information in one of the categories

426 (i.e., animals or faces) can be used to predict decision behaviour, as shown here, then this
427 interpretation needs to be revisited.

428

429 **4.5 Conclusion**

430 In this study, we combined the distance-to-bound approach (Ritchie & Carlson, 2016) with a
431 searchlight decoding analysis to find brain areas with decodable information that is suitable for
432 read-out in behaviour. Our results showed that decodable information is not always equally
433 suitable for read-out by the brain in behaviour. This speaks to the current debate in neuroimaging
434 research about whether the information that we can decode is the same information that is used
435 by the brain in behaviour (de-Wit et al., 2016).

436

437 **References**

- 438 Afraz, S.-R., Kiani, R., & Esteky, H. (2006). Microstimulation of inferotemporal cortex influences
439 face categorization. *Nature*, *442*(7103), 692–695.
- 440 Ashby, F. G. (2000). A Stochastic Version of General Recognition Theory. *Journal of Mathematical*
441 *Psychology*, *44*(2), 310–329. <https://doi.org/10.1006/jmps.1998.1249>
- 442 Ashby, F. G., & Maddox, W. T. (1994). A Response Time Theory of Separability and Integrality in
443 Speeded Classification. *Journal of Mathematical Psychology*, *38*(4), 423–466.
444 <https://doi.org/10.1006/jmps.1994.1032>
- 445 Benjamini, Y., & Hochberg, Y. (1995). Controlling the False Discovery Rate: A Practical and
446 Powerful Approach to Multiple Testing. *Journal of the Royal Statistical Society. Series B*
447 *(Methodological)*, *57*(1), 289–300.
- 448 Bouton, S., Chambon, V., Tyrand, R., Guggisberg, A. G., Seeck, M., Karkar, S., ... Giraud, A.-L. (2018).
449 Focal versus distributed temporal cortex activity for speech sound category assignment.
450 *Proceedings of the National Academy of Sciences*, *115*(6), E1299–E1308.

- 451 Bracci, S., Daniels, N., & Op de Beeck, H. P. (2017). Task Context Overrides Object- and Category-
452 Related Representational Content in the Human Parietal Cortex. *Cerebral Cortex*, 1–12.
453 <https://doi.org/10.1093/cercor/bhw419>
- 454 Bracci, S., & Op de Beeck, H. P. (2016). Dissociations and Associations between Shape and
455 Category Representations in the Two Visual Pathways. *Journal of Neuroscience*, 36(2), 432–
456 444. <https://doi.org/10.1523/JNEUROSCI.2314-15.2016>
- 457 Bugatus, L., Weiner, K. S., & Grill-Spector, K. (2017). Task alters category representations in
458 prefrontal but not high-level visual cortex. *NeuroImage*, 155, 437–449.
459 <https://doi.org/10.1016/j.neuroimage.2017.03.062>
- 460 Caramazza, A., & Shelton, J. R. (1998). Domain-Specific Knowledge Systems in the Brain: The
461 Animate-Inanimate Distinction. *Journal of Cognitive Neuroscience*, 10(1), 1–34.
462 <https://doi.org/10.1162/089892998563752>
- 463 Carlson, T. A., Ritchie, J. B., Kriegeskorte, N., Durvasula, S., & Ma, J. (2014). Reaction Time for
464 Object Categorization Is Predicted by Representational Distance. *Journal of Cognitive
465 Neuroscience*, 26(1), 132–142. https://doi.org/10.1162/jocn_a_00476
- 466 Carlson, T. A., Schrater, P., & He, S. (2003). Patterns of Activity in the Categorical Representations
467 of Objects. *Journal of Cognitive Neuroscience*, 15(5), 704–717.
468 <https://doi.org/10.1162/jocn.2003.15.5.704>
- 469 Carlson, T. A., Tovar, D. A., Alink, A., & Kriegeskorte, N. (2013). Representational dynamics of
470 object vision: The first 1000 ms. *Journal of Vision*, 13(10), 1.
471 <https://doi.org/10.1167/13.10.1>
- 472 Cichy, R. M., Pantazis, D., & Oliva, A. (2014). Resolving human object recognition in space and
473 time. *Nature Neuroscience*, 17(3), 455–462. <https://doi.org/10.1038/nn.3635>

- 474 Cichy, R. M., Pantazis, D., & Oliva, A. (2016). Similarity-Based Fusion of MEG and fMRI Reveals
475 Spatio-Temporal Dynamics in Human Cortex During Visual Object Recognition. *Cerebral*
476 *Cortex*, 26(8), 3563–3579. <https://doi.org/10.1093/cercor/bhw135>
- 477 Cichy, R. M., Sterzer, P., Heinzle, J., Elliott, L. T., Ramirez, F., & Haynes, J.-D. (2013). Probing
478 principles of large-scale object representation: Category preference and location encoding.
479 *Human Brain Mapping*, 34(7), 1636–1651. <https://doi.org/10.1002/hbm.22020>
- 480 Cohen, M. A., Dennett, D. C., & Kanwisher, N. (2016). What is the Bandwidth of Perceptual
481 Experience? *Trends in Cognitive Sciences*, 20(5), 324–335.
482 <https://doi.org/10.1016/j.tics.2016.03.006>
- 483 Cox, D. D., & Savoy, R. L. (2003). Functional magnetic resonance imaging (fMRI) “brain reading”:
484 detecting and classifying distributed patterns of fMRI activity in human visual cortex.
485 *NeuroImage*, 19(2), 261–270. [https://doi.org/10.1016/S1053-8119\(03\)00049-1](https://doi.org/10.1016/S1053-8119(03)00049-1)
- 486 Crouzet, S. M., Kirchner, H., & Thorpe, S. J. (2010). Fast saccades toward faces: Face detection in
487 just 100 ms. *Journal of Vision*, 10(4), 16. <https://doi.org/10.1167/10.4.16>
- 488 Crouzet, S. M., & Thorpe, S. J. (2011). Low-Level Cues and Ultra-Fast Face Detection. *Frontiers in*
489 *Psychology*, 2. <https://doi.org/10.3389/fpsyg.2011.00342>
- 490 de-Wit, L., Alexander, D., Ekroll, V., & Wagemans, J. (2016). Is neuroimaging measuring
491 information in the brain? *Psychonomic Bulletin & Review*, 23(5), 1415–1428.
492 <https://doi.org/10.3758/s13423-016-1002-0>
- 493 DiCarlo, J. J., & Cox, D. D. (2007). Untangling invariant object recognition. *Trends in Cognitive*
494 *Sciences*, 11(8), 333–341. <https://doi.org/10.1016/j.tics.2007.06.010>
- 495 DiCarlo, J. J., Zoccolan, D., & Rust, N. C. (2012). How Does the Brain Solve Visual Object
496 Recognition? *Neuron*, 73(3), 415–434. <https://doi.org/10.1016/j.neuron.2012.01.010>

- 497 Downing, P. E., Chan, A. W.-Y., Peelen, M. V., Dodds, C. M., & Kanwisher, N. (2006). Domain
498 Specificity in Visual Cortex. *Cerebral Cortex*, *16*(10), 1453–1461.
499 <https://doi.org/10.1093/cercor/bhj086>
- 500 Downing, P. E., Jiang, Y., Shuman, M., & Kanwisher, N. (2001). A Cortical Area Selective for Visual
501 Processing of the Human Body. *Science*, *293*(5539), 2470–2473.
502 <https://doi.org/10.1126/science.1063414>
- 503 Downing, P. E., & Peelen, M. V. (2016). Body selectivity in occipitotemporal cortex: Causal
504 evidence. *Neuropsychologia*, *83*, 138–148.
505 <https://doi.org/10.1016/j.neuropsychologia.2015.05.033>
- 506 Duncan, J. (2001). An adaptive coding model of neural function in prefrontal cortex. *Nature*
507 *Reviews Neuroscience*, *2*(11), 820–829.
- 508 Freedman, D. J., & Assad, J. A. (2006). Experience-dependent representation of visual categories in
509 parietal cortex. *Nature*, *443*(7107), 85–88.
- 510 Freedman, D. J., & Assad, J. A. (2016). Neuronal Mechanisms of Visual Categorization: An Abstract
511 View on Decision Making. *Annual Review of Neuroscience*, *39*(1), 129–147.
512 <https://doi.org/10.1146/annurev-neuro-071714-033919>
- 513 Freedman, D. J., Riesenhuber, M., Poggio, T., & Miller, E. K. (2001). Categorical Representation of
514 Visual Stimuli in the Primate Prefrontal Cortex. *Science*, *291*(5502), 312–316.
515 <https://doi.org/10.1126/science.291.5502.312>
- 516 Freedman, D. J., Riesenhuber, M., Poggio, T., & Miller, E. K. (2003). A Comparison of Primate
517 Prefrontal and Inferior Temporal Cortices during Visual Categorization. *The Journal of*
518 *Neuroscience*, *23*(12), 5235–5246.
- 519 Freud, E., Culham, J. C., Plaut, D. C., & Behrmann, M. (2017). The large-scale organization of shape
520 processing in the ventral and dorsal pathways. *ELife*, *6*, e27576.
521 <https://doi.org/10.7554/eLife.27576>

- 522 Green, D. M., & Swets, J. A. (1966). Signal detection theory and psychophysics. *New York*.
- 523 Grill-Spector, K., & Weiner, K. S. (2014). The functional architecture of the ventral temporal cortex
524 and its role in categorization. *Nature Reviews Neuroscience*, *15*(8), 536–548.
525 <https://doi.org/10.1038/nrn3747>
- 526 Grootswagers, T., Kennedy, B. L., Most, S. B., & Carlson, T. A. (2017). Neural signatures of dynamic
527 emotion constructs in the human brain. *Neuropsychologia*.
528 <https://doi.org/10.1016/j.neuropsychologia.2017.10.016>
- 529 Grootswagers, T., Ritchie, J. B., Wardle, S. G., Heathcote, A., & Carlson, T. A. (2017). Asymmetric
530 Compression of Representational Space for Object Animacy Categorization under
531 Degraded Viewing Conditions. *Journal of Cognitive Neuroscience*, *29*(12), 1995–2010.
532 https://doi.org/10.1162/jocn_a_01177
- 533 Grootswagers, T., Wardle, S. G., & Carlson, T. A. (2017). Decoding Dynamic Brain Patterns from
534 Evoked Responses: A Tutorial on Multivariate Pattern Analysis Applied to Time Series
535 Neuroimaging Data. *Journal of Cognitive Neuroscience*, *29*(4), 677–697.
536 https://doi.org/10.1162/jocn_a_01068
- 537 Haushofer, J., Livingstone, M. S., & Kanwisher, N. (2008). Multivariate Patterns in Object-Selective
538 Cortex Dissociate Perceptual and Physical Shape Similarity. *PLOS Biology*, *6*(7), e187.
539 <https://doi.org/10.1371/journal.pbio.0060187>
- 540 Haxby, J. V., Gobbini, M. I., Furey, M. L., Ishai, A., Schouten, J. L., & Pietrini, P. (2001). Distributed
541 and Overlapping Representations of Faces and Objects in Ventral Temporal Cortex. *Science*,
542 *293*(5539), 2425–2430. <https://doi.org/10.1126/science.1063736>
- 543 Haynes, J.-D. (2015). A Primer on Pattern-Based Approaches to fMRI: Principles, Pitfalls, and
544 Perspectives. *Neuron*, *87*(2), 257–270. <https://doi.org/10.1016/j.neuron.2015.05.025>

- 545 Haynes, J.-D., Sakai, K., Rees, G., Gilbert, S., Frith, C., & Passingham, R. E. (2007). Reading Hidden
546 Intentions in the Human Brain. *Current Biology*, *17*(4), 323–328.
547 <https://doi.org/10.1016/j.cub.2006.11.072>
- 548 Hebart, M. N., & Baker, C. I. (2017). Deconstructing multivariate decoding for the study of brain
549 function. *NeuroImage*. <https://doi.org/10.1016/j.neuroimage.2017.08.005>
- 550 Honey, C., Kirchner, H., & VanRullen, R. (2008). Faces in the cloud: Fourier power spectrum biases
551 ultrarapid face detection. *Journal of Vision*, *8*(12), 9–9. <https://doi.org/10.1167/8.12.9>
- 552 Hong, H., Yamins, D. L. K., Majaj, N. J., & DiCarlo, J. J. (2016). Explicit information for category-
553 orthogonal object properties increases along the ventral stream. *Nature Neuroscience*,
554 *19*(4), 613–622. <https://doi.org/10.1038/nn.4247>
- 555 Hung, C. P., Kreiman, G., Poggio, T., & DiCarlo, J. J. (2005). Fast Readout of Object Identity from
556 Macaque Inferior Temporal Cortex. *Science*, *310*(5749), 863–866.
557 <https://doi.org/10.1126/science.1117593>
- 558 Jackson, J., Rich, A. N., Williams, M. A., & Woolgar, A. (2016). Feature-selective Attention in
559 Frontoparietal Cortex: Multivoxel Codes Adjust to Prioritize Task-relevant Information.
560 *Journal of Cognitive Neuroscience*, *29*(2), 310–321. https://doi.org/10.1162/jocn_a_01039
- 561 Jeong, S. K., & Xu, Y. (2016). Behaviorally Relevant Abstract Object Identity Representation in the
562 Human Parietal Cortex. *Journal of Neuroscience*, *36*(5), 1607–1619.
563 <https://doi.org/10.1523/JNEUROSCI.1016-15.2016>
- 564 Kaiser, D., Azzalini, D. C., & Peelen, M. V. (2016). Shape-independent object category responses
565 revealed by MEG and fMRI decoding. *Journal of Neurophysiology*, *115*(4), 2246–2250.
566 <https://doi.org/10.1152/jn.01074.2015>
- 567 Kamitani, Y., & Tong, F. (2005). Decoding the visual and subjective contents of the human brain.
568 *Nature Neuroscience*, *8*(5), 679–685. <https://doi.org/10.1038/nn1444>

- 569 Kanwisher, N., McDermott, J., & Chun, M. M. (1997). The Fusiform Face Area: A Module in Human
570 Extrastriate Cortex Specialized for Face Perception. *The Journal of Neuroscience*, *17*(11),
571 4302–4311.
- 572 Kiani, R., Cueva, C. J., Reppas, J. B., & Newsome, W. T. (2014). Dynamics of Neural Population
573 Responses in Prefrontal Cortex Indicate Changes of Mind on Single Trials. *Current Biology*,
574 *24*(13), 1542–1547. <https://doi.org/10.1016/j.cub.2014.05.049>
- 575 Kirchner, H., & Thorpe, S. J. (2006). Ultra-rapid object detection with saccadic eye movements:
576 Visual processing speed revisited. *Vision Research*, *46*(11), 1762–1776.
577 <https://doi.org/10.1016/j.visres.2005.10.002>
- 578 Konen, C. S., & Kastner, S. (2008). Two hierarchically organized neural systems for object
579 information in human visual cortex. *Nature Neuroscience*, *11*(2), 224–231.
580 <https://doi.org/10.1038/nn2036>
- 581 Krakauer, J. W., Ghazanfar, A. A., Gomez-Marín, A., MacIver, M. A., & Poeppel, D. (2017).
582 Neuroscience Needs Behavior: Correcting a Reductionist Bias. *Neuron*, *93*(3), 480–490.
583 <https://doi.org/10.1016/j.neuron.2016.12.041>
- 584 Kriegeskorte, N., Goebel, R., & Bandettini, P. A. (2006). Information-based functional brain
585 mapping. *Proceedings of the National Academy of Sciences of the United States of America*,
586 *103*(10), 3863–3868. <https://doi.org/10.1073/pnas.0600244103>
- 587 Kriegeskorte, N., Mur, M., Ruff, D. A., Kiani, R., Bodurka, J., Esteky, H., ... Bandettini, P. A. (2008).
588 Matching Categorical Object Representations in Inferior Temporal Cortex of Man and
589 Monkey. *Neuron*, *60*(6), 1126–1141. <https://doi.org/10.1016/j.neuron.2008.10.043>
- 590 Long, B., Yu, C.-P., & Konkle, T. (2017). A mid-level organization of the ventral stream. *BioRxiv*,
591 213934. <https://doi.org/10.1101/213934>

- 592 McKee, J. L., Riesenhuber, M., Miller, E. K., & Freedman, D. J. (2014). Task dependence of visual
593 and category representations in prefrontal and inferior temporal cortices. *Journal of*
594 *Neuroscience*, 34(48), 16065–16075.
- 595 Mur, M., Meys, M., Bodurka, J., Goebel, R., Bandettini, P. A., & Kriegeskorte, N. (2013). Human
596 Object-Similarity Judgments Reflect and Transcend the Primate-IT Object Representation.
597 *Frontiers in Psychology*, 4. <https://doi.org/10.3389/fpsyg.2013.00128>
- 598 Naselaris, T., Kay, K. N., Nishimoto, S., & Gallant, J. L. (2011). Encoding and decoding in fMRI.
599 *NeuroImage*, 56(2), 400–410. <https://doi.org/10.1016/j.neuroimage.2010.07.073>
- 600 Oosterhof, N. N., Connolly, A. C., & Haxby, J. V. (2016). CoSMoMVPA: Multi-Modal Multivariate
601 Pattern Analysis of Neuroimaging Data in Matlab/GNU Octave. *Frontiers in*
602 *Neuroinformatics*, 27. <https://doi.org/10.3389/fninf.2016.00027>
- 603 Pereira, F., Mitchell, T., & Botvinick, M. (2009). Machine learning classifiers and fMRI: A tutorial
604 overview. *NeuroImage*, 45(1, Supplement 1), S199–S209.
605 <https://doi.org/10.1016/j.neuroimage.2008.11.007>
- 606 Philiastides, M. G., & Sajda, P. (2006). Temporal Characterization of the Neural Correlates of
607 Perceptual Decision Making in the Human Brain. *Cerebral Cortex*, 16(4), 509–518.
608 <https://doi.org/10.1093/cercor/bhi130>
- 609 Proklova, D., Kaiser, D., & Peelen, M. V. (2016). Disentangling Representations of Object Shape and
610 Object Category in Human Visual Cortex: The Animate–Inanimate Distinction. *Journal of*
611 *Cognitive Neuroscience*, 1–13. https://doi.org/10.1162/jocn_a_00924
- 612 Raizada, R. D. S., Tsao, F.-M., Liu, H.-M., & Kuhl, P. K. (2010). Quantifying the Adequacy of Neural
613 Representations for a Cross-Language Phonetic Discrimination Task: Prediction of
614 Individual Differences. *Cerebral Cortex*, 20(1), 1–12.
615 <https://doi.org/10.1093/cercor/bhp076>

- 616 Riesenhuber, M., & Poggio, T. (1999). Hierarchical models of object recognition in cortex. *Nature*
617 *Neuroscience*, 2(11), 1019–1025.
- 618 Ritchie, J. B., & Carlson, T. A. (2016). Neural Decoding and “Inner” Psychophysics: A Distance-to-
619 Bound Approach for Linking Mind, Brain, and Behavior. *Frontiers in Neuroscience*, 190.
620 <https://doi.org/10.3389/fnins.2016.00190>
- 621 Ritchie, J. B., Kaplan, D. M., & Klein, C. (2017). Decoding the Brain: Neural Representation and the
622 Limits of Multivariate Pattern Analysis in Cognitive Neuroscience. *The British Journal for the*
623 *Philosophy of Science*. <https://doi.org/10.1093/bjps/axx023>
- 624 Ritchie, J. B., Tovar, D. A., & Carlson, T. A. (2015). Emerging Object Representations in the Visual
625 System Predict Reaction Times for Categorization. *PLoS Comput Biol*, 11(6), e1004316.
626 <https://doi.org/10.1371/journal.pcbi.1004316>
- 627 Schwarzlose, R. F., Swisher, J. D., Dang, S., & Kanwisher, N. (2008). The distribution of category and
628 location information across object-selective regions in human visual cortex. *Proceedings of*
629 *the National Academy of Sciences*, 105(11), 4447–4452.
630 <https://doi.org/10.1073/pnas.0800431105>
- 631 Sereno, A. B., & Maunsell, J. H. R. (1998). Shape selectivity in primate lateral intraparietal cortex.
632 *Nature*, 395(6701), 500–503. <https://doi.org/10.1038/26752>
- 633 Silver, M. A., & Kastner, S. (2009). Topographic maps in human frontal and parietal cortex. *Trends*
634 *in Cognitive Sciences*, 13(11), 488–495. <https://doi.org/10.1016/j.tics.2009.08.005>
- 635 Thorpe, S., Fize, D., & Marlot, C. (1996). Speed of processing in the human visual system. *Nature*,
636 381(6582), 520–522.
- 637 Ungerleider, L. G., & Mishkin, M. (1982). Two cortical visual systems. *Analysis of Visual Behavior*,
638 549–586.

- 639 van Bergen, R. S., Ji Ma, W., Pratte, M. S., & Jehee, J. F. M. (2015). Sensory uncertainty decoded
640 from visual cortex predicts behavior. *Nature Neuroscience*, *18*(12), 1728–1730.
641 <https://doi.org/10.1038/nn.4150>
- 642 Walther, D. B., Caddigan, E., Fei-Fei, L., & Beck, D. M. (2009). Natural Scene Categories Revealed in
643 Distributed Patterns of Activity in the Human Brain. *Journal of Neuroscience*, *29*(34),
644 10573–10581. <https://doi.org/10.1523/JNEUROSCI.0559-09.2009>
- 645 Wang, L., Mruczek, R. E. B., Arcaro, M. J., & Kastner, S. (2015). Probabilistic Maps of Visual
646 Topography in Human Cortex. *Cerebral Cortex*, *25*(10), 3911–3931.
647 <https://doi.org/10.1093/cercor/bhu277>
- 648 Wardle, S. G., Kriegeskorte, N., Grootswagers, T., Khaligh-Razavi, S.-M., & Carlson, T. A. (2016).
649 Perceptual similarity of visual patterns predicts dynamic neural activation patterns
650 measured with MEG. *NeuroImage*, *132*, 59–70.
651 <https://doi.org/10.1016/j.neuroimage.2016.02.019>
- 652 Williams, M. A., Dang, S., & Kanwisher, N. G. (2007). Only some spatial patterns of fMRI response
653 are read out in task performance. *Nature Neuroscience*, *10*(6), 685–686.
654 <https://doi.org/10.1038/nn1900>
- 655 Woolgar, A., Golland, P., & Bode, S. (2014). Coping with confounds in multivoxel pattern analysis:
656 What should we do about reaction time differences? A comment on Todd, Nystrom &
657 Cohen 2013. *NeuroImage*, *98*, 506–512.
658 <https://doi.org/10.1016/j.neuroimage.2014.04.059>
- 659 Woolgar, A., Jackson, J., & Duncan, J. (2016). Coding of Visual, Auditory, Rule, and Response
660 Information in the Brain: 10 Years of Multivoxel Pattern Analysis. *Journal of Cognitive
661 Neuroscience*, *28*(10), 1433–1454. https://doi.org/10.1162/jocn_a_00981

662 Wu, C.-T., Crouzet, S. M., Thorpe, S. J., & Fabre-Thorpe, M. (2015). At 120 msec You Can Spot the
663 Animal but You Don't Yet Know It's a Dog. *Journal of Cognitive Neuroscience*, 27(1), 141–
664 149. https://doi.org/10.1162/jocn_a_00701

665